

Supporting information

Hybrid CsPbBr₃ Superlattice/Ag Microcavity Enabling Strong Exciton–Photon Coupling for Low-Threshold Continuous-Wave Pumped Polariton Lasing

Zhenxu Lin^{a, b}, Rui Huang^{*, a}, Shulei Li^{†, c}, Mingcheng Panmai^d, Yi Zhang^a, Haixia Wu^a, Jie Song^a,
Zewen Lin^a, Hongliang Li^a, and Sheng Lan^{‡, b}

^a School of Material Science and Engineering, Hanshan Normal University, Chaozhou 521041, China

^b Guangdong Provincial Key Laboratory of Nanophotonic Functional Materials and Devices, School of Information and Optoelectronic Science and Engineering, South China Normal University, Guangzhou 510006, China

^c School of Optoelectronic Engineering, Guangdong Polytechnic Normal University, Guangzhou 510665, China

^d Division of Physics and Applied Physics, School of Physical and Mathematical Sciences, Nanyang Technological University; Singapore, 637371, Singapore

* Corresponding author : rhuang@hstc.edu.cn

† Corresponding author : shuleili@gpnu.edu.cn

‡ Corresponding author : slan@scnu.edu.cn

Experimental Section

Fabrication of CsPbBr₃ QDs

In this work, CsPbBr₃ QDs were synthesized by hot-injection method. Cesium carbonate (Cs₂CO₃, Aladdin, 99.99%), lead(II) bromide (PbBr₂, Aladdin, 99.99%), oleic acid (OA, Aladdin, 90%), oleyamine (OAm, Aladdin, 90%), and octadecene (ODE, Aladdin, 95%) were used as the reactant precursors. First, Cs-oleate precursors were fabricated according to a typical synthesis. 100 mg Cs₂CO₃, 1 mL OA were mixed with 10 mL ODE in a 100 mL three-neck flask. 276 mg PbBr₂, 2 mL OA, and 2 mL OAm were mixed with 20 mL ODE in another 100 mL three-neck flask. Then, the above solutions were maintained at 90 °C for 30 min under vacuum in order to remove air and moisture and then heated to 120 °C for 60 min until the Cs-oleate/Pb-oleate is completely dissolved in ODE. After that, the temperature of Cs-oleate solution was kept at 120 °C under nitrogen atmosphere for further hot injection, while the temperature of Pb-oleate solution was gradually increased to 180 °C under nitrogen atmosphere and kept for 20 min. Subsequently, 2 mL hot Cs-oleate solution was swiftly injected into the Pb-oleate solution. After 5s, the reaction mixture was immediately cooled down in an ice-water bath. The crude CsPbBr₃ QDs solution was centrifuged at 9200 rpm for 5 min. The precipitate was dispersed with a mixture of hexane and acetone with a volume ratio of 1:1 and then centrifuged at 8800 rpm for 5 min. The final CsPbBr₃ QDs supernatant was dissolved in the hexane solution.

Synthesis of CsPbBr₃ SL/Ag hybrid microcavities

The CsPbBr₃ SLs are synthesized by using acetone-assisted self-assembly of CsPbBr₃ QDs. The as-prepared CsPbBr₃ QDs solution, to which acetone was added, was allowed to stand at room temperature for 7 days (see Figure S1 (a)). The regulation of the size of CsPbBr₃ SLs can be achieved by adjusting the ratio of acetone to hexane. As shown in Figure S1 (c)-(e), the side length L of CsPbBr₃ SLs increase with increasing the ratio of acetone to hexane. Then 50 μL solution was spin-coated onto a 10*10 mm clean Ag/SiO₂ substrate at a rate of 4000 rpm for 30 s. The CsPbBr₃ SLs were form on the surface of Ag film. In order to prevent the oxidation surface of the Ag film, a 5-nm-thick SnO₂ was coated on the Ag film as an anti-oxidation layer. After that, the substrates were dried in a vacuum oven for 12 hours in ambient condition.

Characterization of CsPbBr₃ QDs and CsPbBr₃ SLs/Ag hybrid microcavities

The morphology and component elements of CsPbBr₃ SLs were characterized by a scanning electron

microscope (SEM) (Hitachi SU 5000), a high-resolution transmission electron microscope (HR-TEM) (JEM-1400 PLUS) and energy dispersive spectroscopy (EDS) (Bruker EDS QUANTAX), respectively. The crystal structures of CsPbBr₃ QDs and SLs were characterized by X-ray diffraction (XRD) (Bruker D8 Advance) at 35 kV and 35 mA. The local atomic environment and bonding configuration of SLs were measured by using Raman spectrometer equipped with a 633-nm laser (Horiba LabRAM HR Evolution). The UV-Vis absorption spectra were measured by using a spectrophotometer (Shimadzu UV-Vis 3600) (the absorption spectrum is shown in Figure S1 (b)). The PL spectra of CsPbBr₃ SCs were collected by a 50× objective lens in a Raman spectrometer system (Horiba LabRAM HR Evolution) equipped with a 405-nm laser (Changchun New Industries Optoelectronic Tech Co., Ltd.).

Optical Characterization of CsPbBr₃ SL/Ag hybrid microcavities

The 800nm femtosecond laser light (Mira 900S, Coherent, 130 fs) was employed to excite CsPbBr₃ SLs, a high repetition rate 76 MHz was measure luminesure and power-dependent, and a low repetition rate of 3.8 MHz (obtained by using a pulse picker) and a time-correlated single photon system (lifespec II, Edinburgh Instruments) was employed to measure luminescence lifetimes. The single-mode lasing spectra measurement were performed by using 400 nm femtosecond pulses of 1 kHz (Legend, Coherent). A 405nm CW laser was measured multimode lasing spectra. The scattering light and photoluminescence were collected by using a conventional dark-field microscope (Observer A1, Zeiss) equipped with a spectrometer (SR-500i-B1, Andor) and a coupled-charge device (DU970N-BV, Andor).

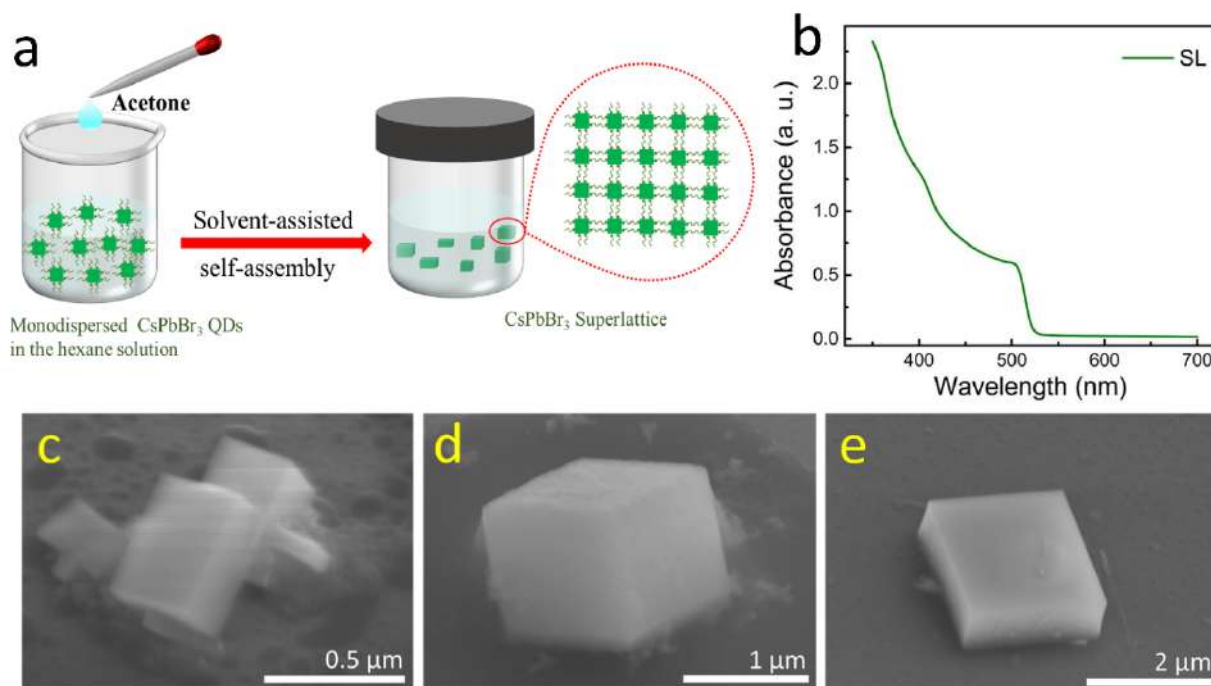


Figure S1 (a) Schematics of the fabrication process of CsPbBr₃ SLs prepared by polar solvent (acetone)-assisted self-assembly of monodispersed QDs in hexane solution. (b) The absorption spectrum of the CsPbBr₃ SL. SEM image of CsPbBr₃ SLs prepared by different volume ratio of hexane/ acetone: 4:1 (c), 2:1 (d), and 1: 1(e).

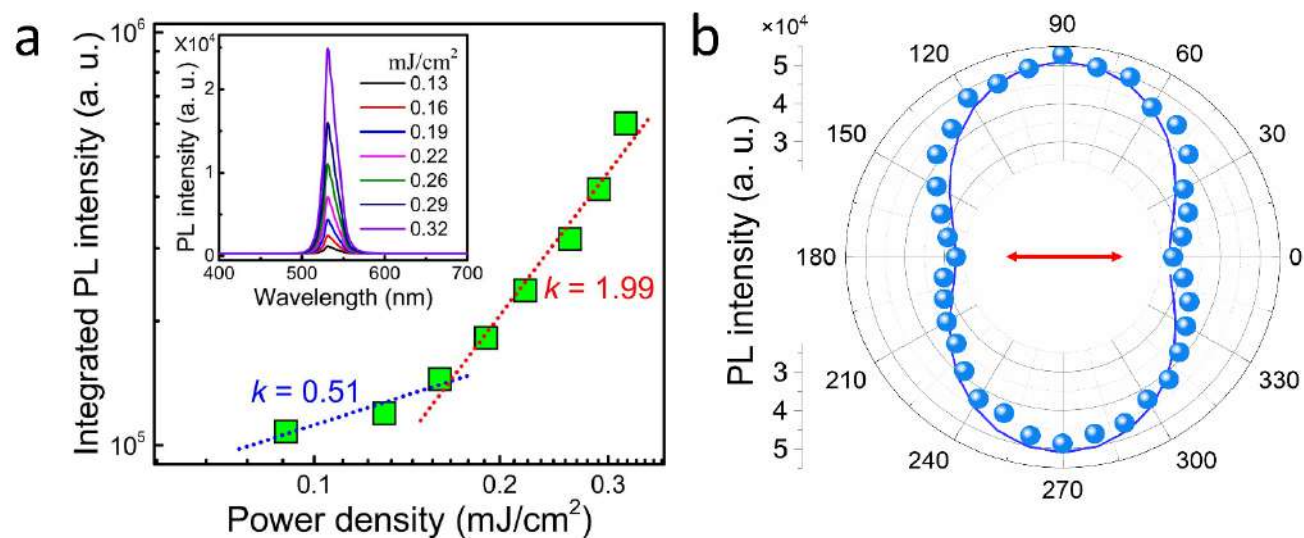


Figure S2 (a) The dependence of the integrated PL intensity on the excitation power density for a CsPbBr₃ SL. The inset shows PL spectra measured for a CsPbBr₃ SL excited by using 800-nm femtosecond laser pulses of 76 MHz at different laser powers. (b) The dependence of the integrated emission intensity on the detection polarization angle for a CsPbBr₃ SL. The degree of polarization (DOP) can be defined as $DOP = (I_{max} - I_{min}) / (I_{max} + I_{min})$ [1], and the value is calculated as 0.33.

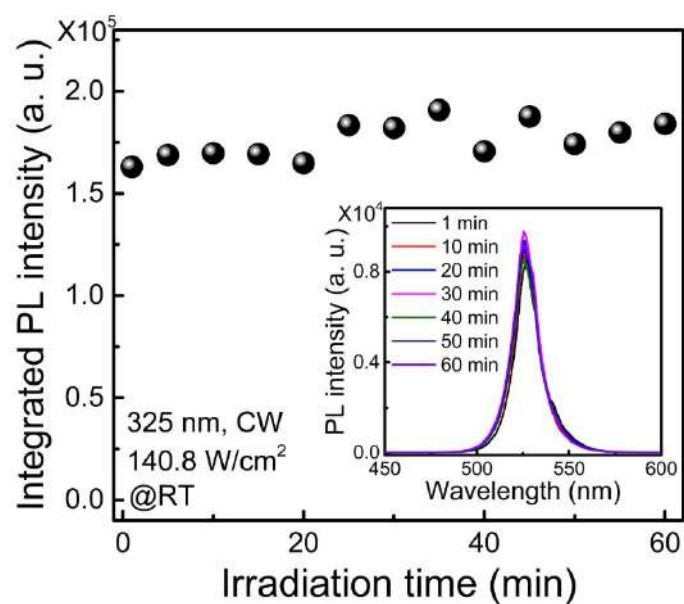


Figure S3 Integrated PL intensity of the CsPbBr₃ SL versus continuous 325 nm laser (power density: 140.8W/cm²) illumination time with the inset showing the corresponding PL spectra.

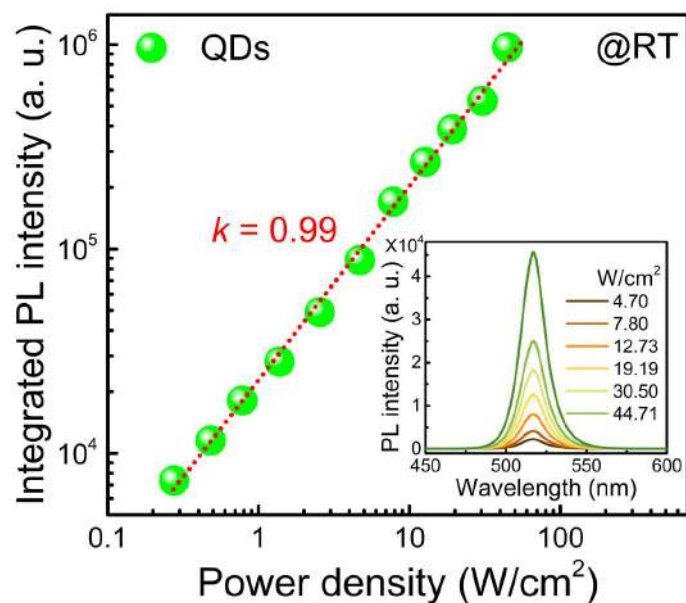


Figure S4 L-L plot of the excitation power density-dependent integrated PL intensity of CsPbBr₃ QDs film. The inset shows the excitation power -dependent PL spectra of CsPbBr₃ QDs film.

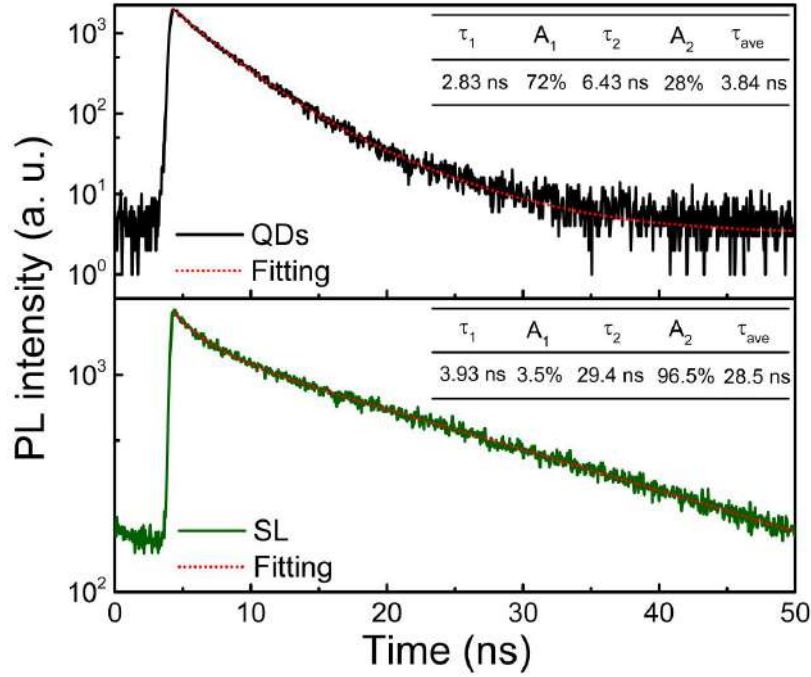


Figure S5 PL decay of CsPbBr₃ QDs film and a SL placed on the Ag film by using the 800 nm femtosecond laser pulses of 3.8 MHz at a low excitation fluence of 0.7 mJ cm⁻². The decay traces were fitted by the biexponential decay function: $I(t) = I_0 + I_1 \exp(-t/\tau_1) + I_2 \exp(-t/\tau_2)$, where I_0 is the background level, I_i and τ_i ($i = 1, 2$) are the amplitude and lifetime of each exponential decay component, respectively. The fast decay component τ_1 can be correlated with carrier decay time influenced by non-radiative defects while the slow decay component τ_2 is correlated with the radiative recombination process [2]. The average decay lifetime was calculated from the following equation: $(I_1 \tau_1^2 + I_2 \tau_2^2) / (I_1 \tau_1 + I_2 \tau_2)$. It is noteworthy that the weight ratio (96.5%) of slow decay component τ_2 in the CsPbBr₃ SL is greatly enhanced with respect to that (28%) in the CsPbBr₃ QDs film. This indicates that the enhancement of radiative recombination rate in the SLs compared to CsPbBr₃ QDs film.

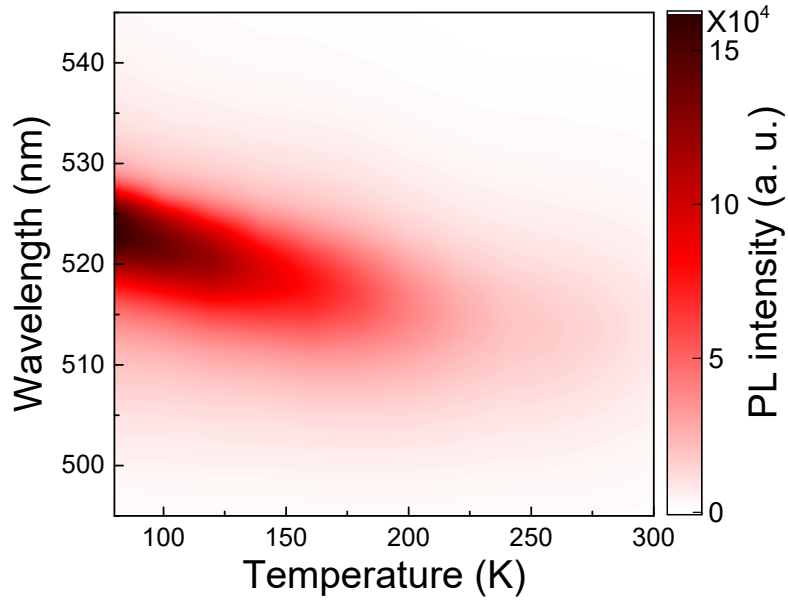


Figure S6 Temperature-dependent PL spectra of CsPbBr₃ QDs measured at various temperatures from 80 to 300 K.

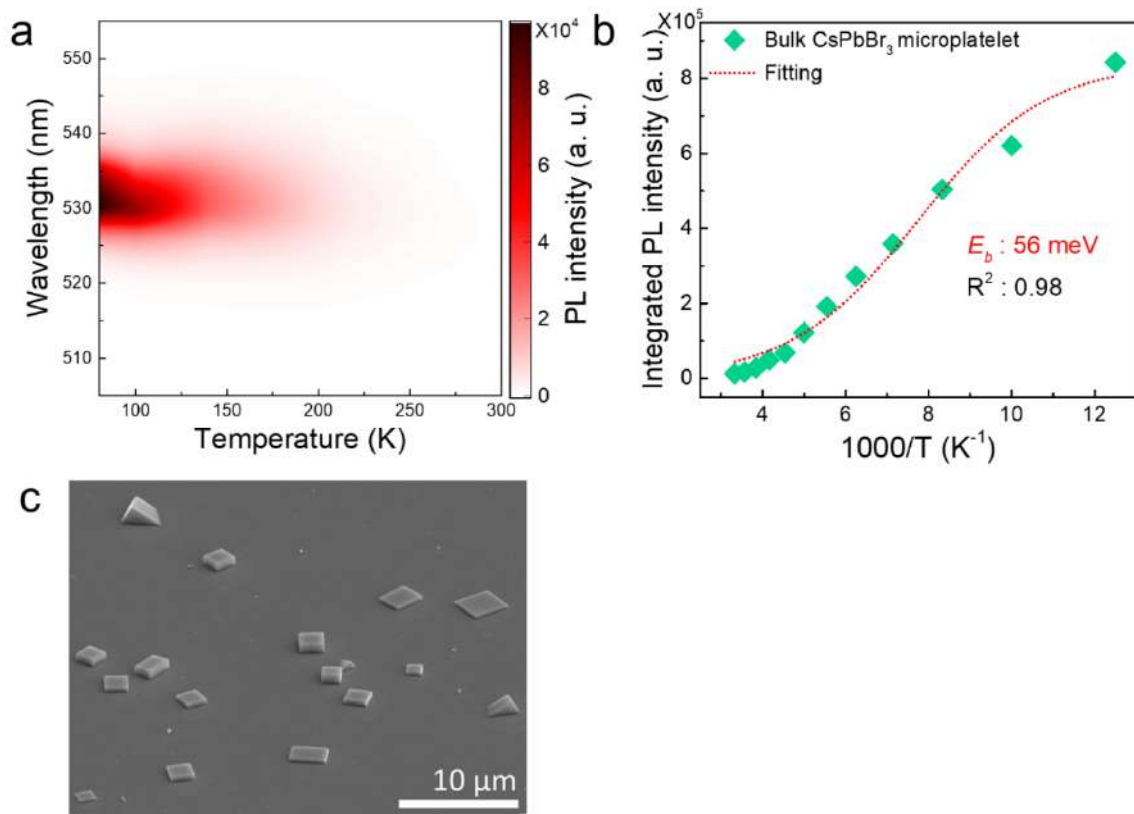


Figure S7 (a) Temperature-dependent PL spectra of a bulk CsPbBr₃ microplatelet measured at various temperatures from 80 to 300 K. (b) Integrated PL intensity of a bulk CsPbBr₃ microplatelet as the function of temperature. (c) The SEM image of bulk CsPbBr₃ microplatelets.

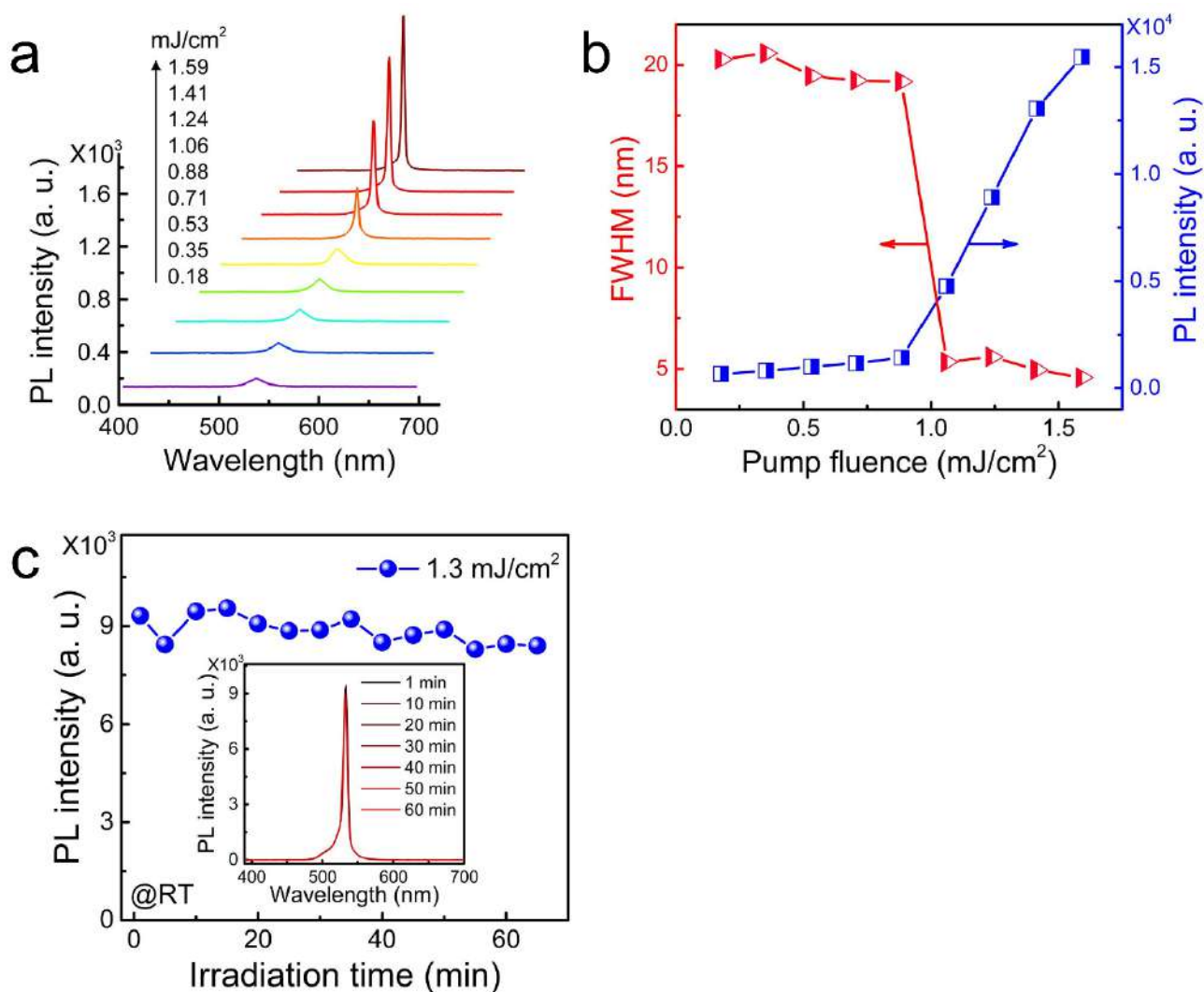


Figure S8 (a) Excitation power-dependent PL spectra of a CsPbBr₃ SL excited by using 800-nm femtosecond laser pulses of 1 kHz at room temperature. (b) The variation tendency of PL intensity and FWHM of a CsPbBr₃ SL with increasing pump fluence. (c) Integrated PL intensities of a CsPbBr₃ SL during subsequent continuous light illumination by a pulsed laser with a pump fluence of 1.45 P_{th}. The inset shows the PL spectra measured at different times.

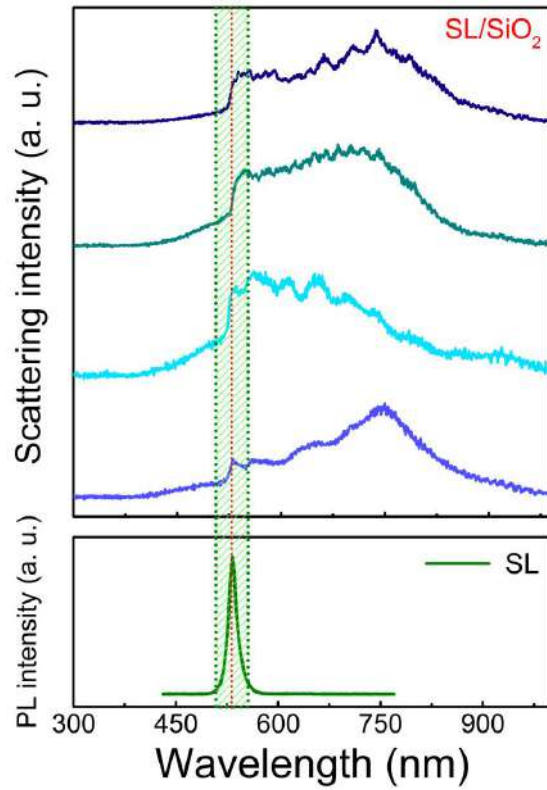


Figure S9 The figure above shows the forward scattering spectra of CsPbBr₃ SLs placed on an SiO₂ substrate though ortho-check by using polarized white light. The figure below shows the PL spectrum of a CsPbBr₃ SL excited under 405 nm CW laser at RT.

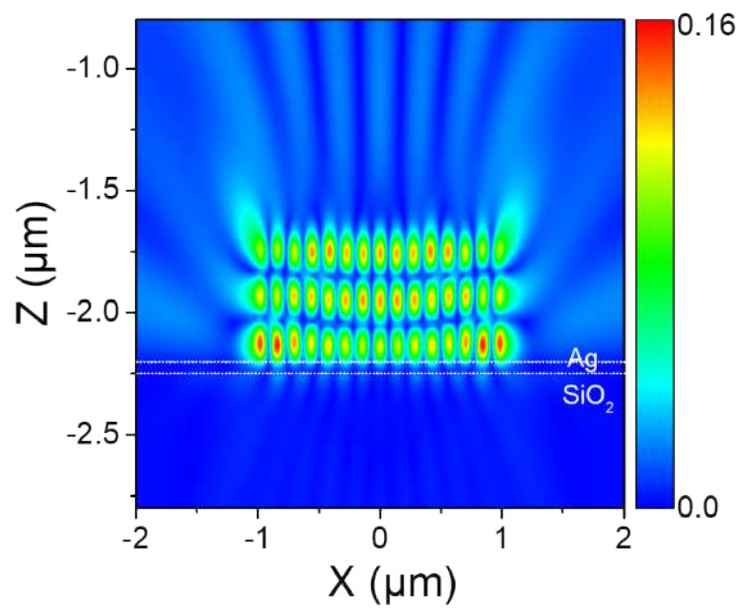


Figure S10 Electric field distributions in the xz plane calculated at 530 nm for a CsPbBr₃ SL placed on an Ag/SiO₂ substrate.

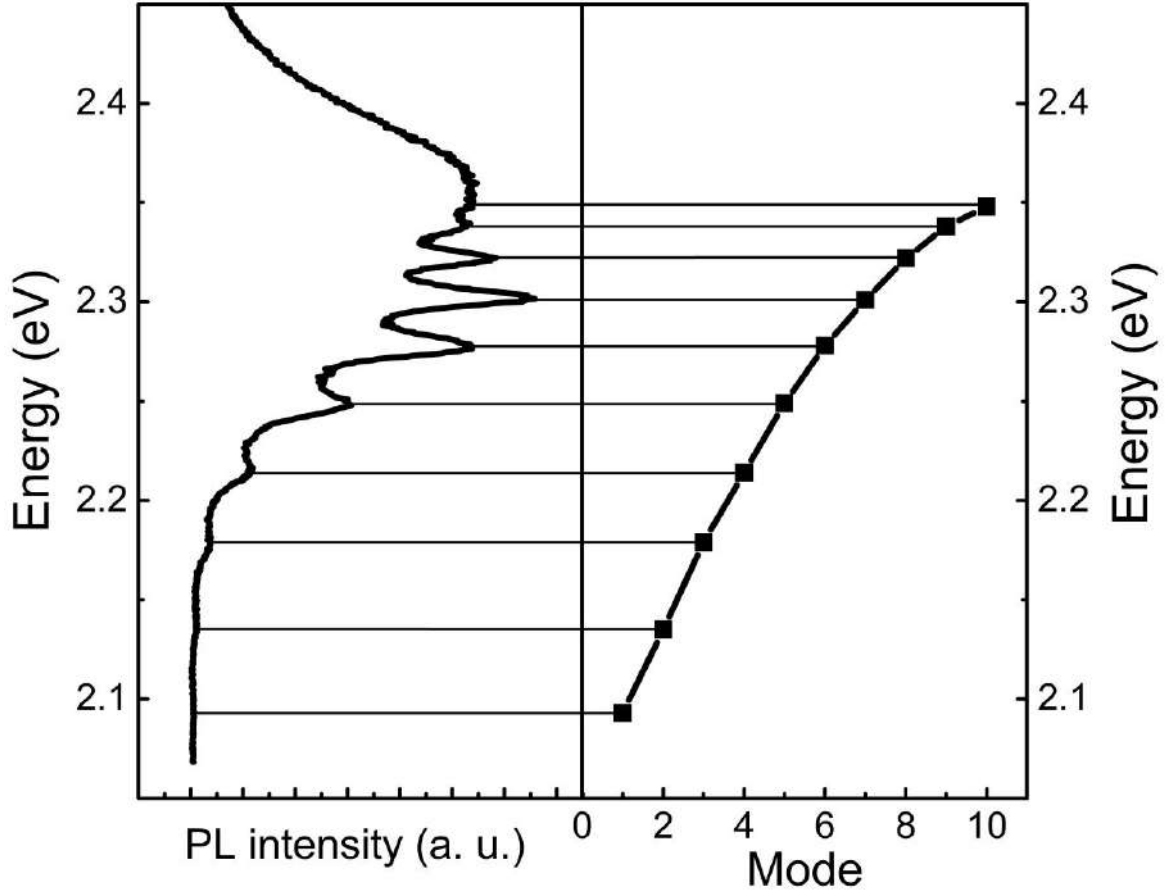


Figure S11 Left panel: The PL spectrum of CsPbBr₃ SLs with $L = 5 \mu\text{m}$ placed on an Ag/SiO₂ substrate under the non-resonant excitation of 405 nm CW laser at RT. Right panel: Polariton mode energies, extracted by a Lorentzian deconvolution of the PL, plotted versus mode number.

In our case, the in-plane wavevector of the polaritons is approximately equal to that of the cavity photons, as shown in Figure 3(d). Thus, the in-plane momentum of the polaritons can be extracted from the dispersion relation of the cavity photons. For the SLs studied in this work, the dominant optical mode in a SL is the WGM supported by the four facets of the SL. It is quite similar to the one-dimensional cavity mode reported previously in nanowires [3]. Thus, the wavevector k of the photons is restricted to integer multiples of $\pi/2\sqrt{2}L$ based on the boundary conditions. In the revised manuscript, we have added a brief discussion on this issue. In each case, the polariton dispersion in the lower polariton band (LPB) can be expressed as follows [1]:

$$E_- = \frac{1}{2}(E_{ex} + E_{ph}) - \frac{1}{2}\sqrt{(E_{ex} - E_{ph})^2 + \Omega^2} \quad (1)$$

Here, Ω is the Rabi splitting energy, E_{ex} is the exciton dispersion and E_{ph} is the cavity photon dispersion, which can be approximated by

$$E_{ph} = \frac{c}{n} \sqrt{\hbar^2 k^2 + m_0 \left(\frac{c}{n}\right)^2} \quad (2)$$

where c , n and \hbar is the speed of light, refractive index and Planck's constant, respectively. k is the wavevector approximated by the in-plane component of the photon wavevector $k_{||} = \pi j / 2\sqrt{2}L + k_0$ and j ($= 0, 1, 2, \dots$) is the mode index from the experimental data, m_0 is the cavity photon mass, which can be approximated by

$$m_0 = \sqrt{2} \frac{\pi n \hbar}{ca} \quad (3)$$

where a is the average cross-sectional dimension of the SL.

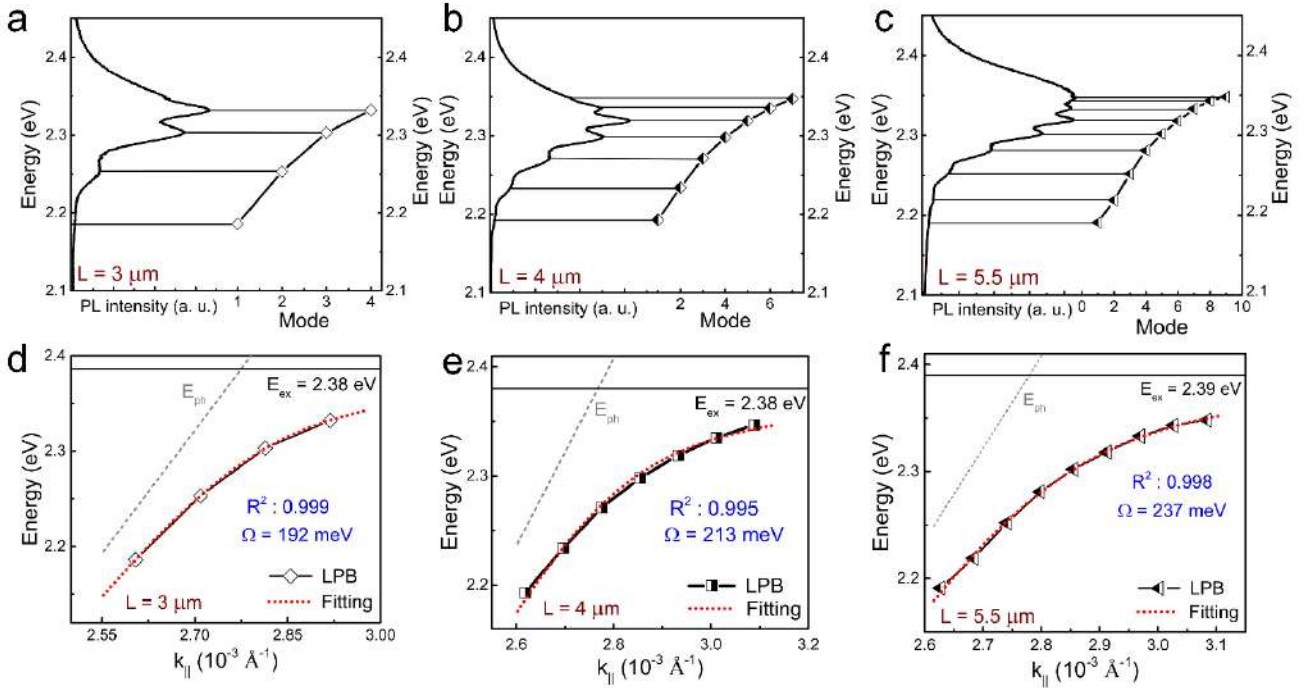


Figure S12 Left panel: PL spectra of CsPbBr₃ SLs with $L = 3 \mu\text{m}$ (a) , $4 \mu\text{m}$ (b) and $5.5 \mu\text{m}$ (c) placed on a Ag/SiO₂ substrate under the excitation of 405-nm CW laser light at RT. Right panel: Resonant energies of the polariton modes extracted from the fitting of the PL spectra by using Lorentz lineshapes. Dispersion relations of the polaritons derived for CsPbBr₃ SLs with $L = 4 \mu\text{m}$ (d), $4 \mu\text{m}$ (e) and $5.5 \mu\text{m}$ (f).

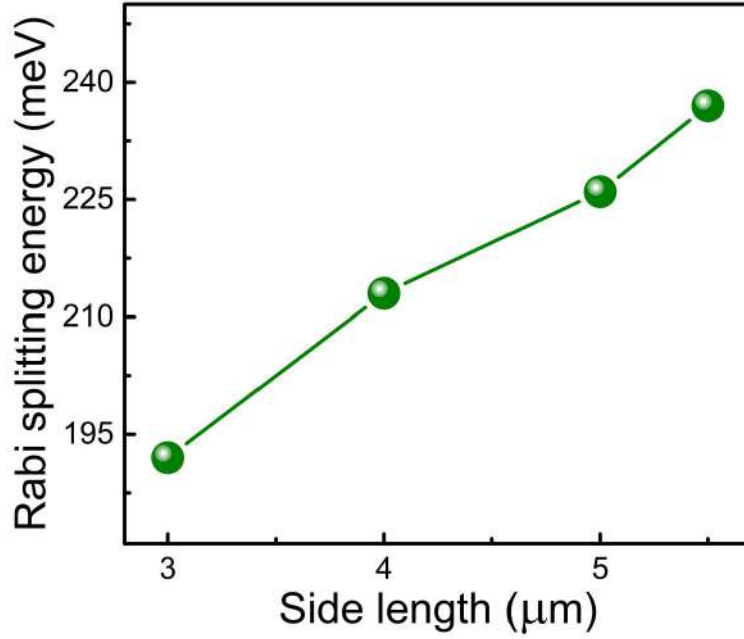
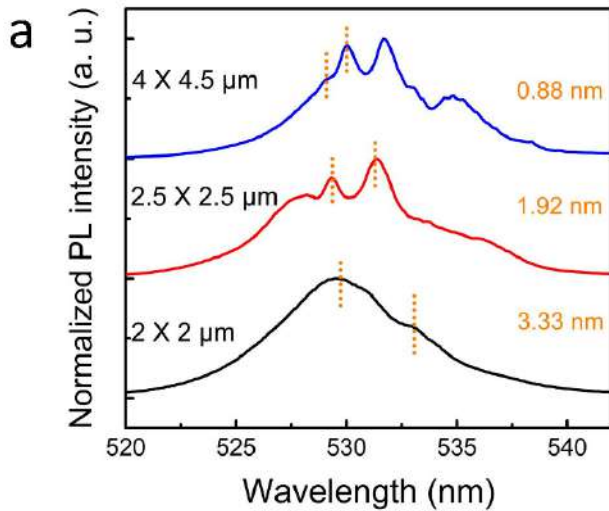


Figure S13 Dependence of the Rabi splitting energy on the side length observed for CsPbBr₃ SLs with different sizes.



b

L(μm)	λ(nm)	FSR(nm)	n _g
2	529.7	3.33	14.9
2.5	529.4	1.92	20.6
4.25	529.1	0.88	26.4

Figure S14 (a) The PL spectra of CsPbBr₃ SLs with L ranging from 2 to 6 μm under an excitation of 405 nm CW laser with power density of 528 W/cm² at 80K. (b) Calculated n_g versus L, based on the whispering-gallery-mode cavity characteristic. The n_g was calculated from $n_g = \lambda^2 / (2\sqrt{2} * L * FSR)$ [4].

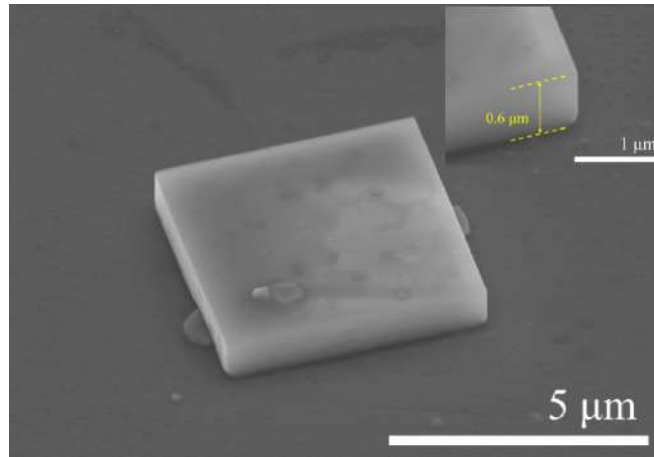


Figure S15 The SEM image of a CsPbBr₃ SL with L = 4.5 μm on a Ag film surface. The inset shows the thickness of a CsPbBr₃ SL.

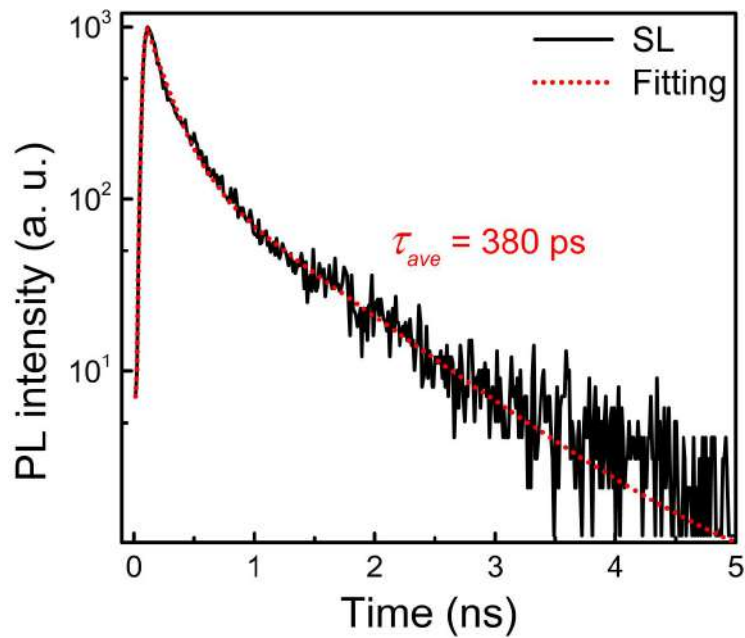


Figure S16 PL decay of a SL placed on the Ag film by using the 800 nm femtosecond laser pulses of 3.8 MHz at a low excitation fluence of 10 mJ cm⁻². The decay traces were fitted by the double exponential decay function: $I(t) = I_0 + I_1 \cdot \exp(-t/\tau_1) + I_2 \cdot \exp(-t/\tau_2)$, where I_0 is the background level, I_i and τ_i ($i = 1, 2$) are the amplitude and lifetime of each exponential decay component, respectively. The average decay lifetime was calculated from the following equation: $(I_1 \cdot \tau_1^2 + I_2 \cdot \tau_2^2) / (I_1 \cdot \tau_1 + I_2 \cdot \tau_2)$ [2].

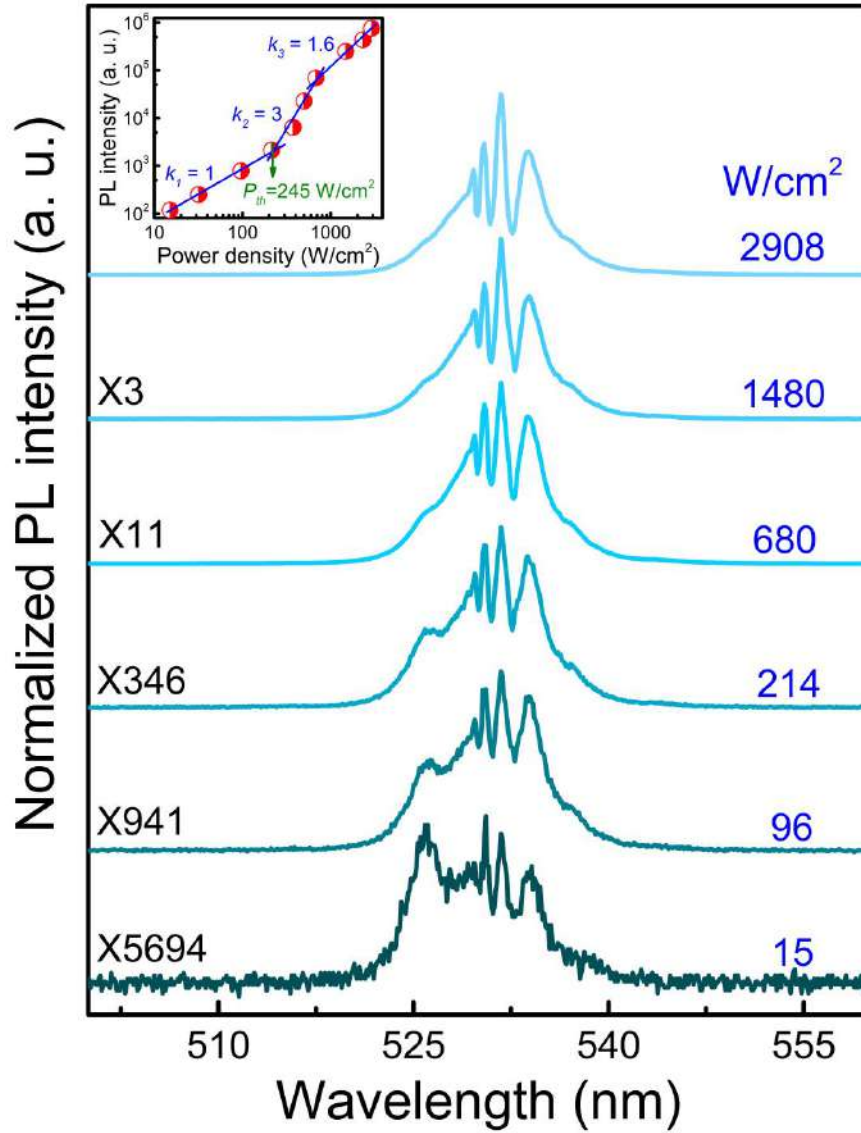


Figure S17 PL spectra measured at different excitation power densities for the CsPbBr₃ SL with $L = 4.5 \mu\text{m}$. The inset shows dependence of the PL intensity on the excitation power density observed for the CsPbBr₃ SLs with $L = 4.5 \mu\text{m}$.

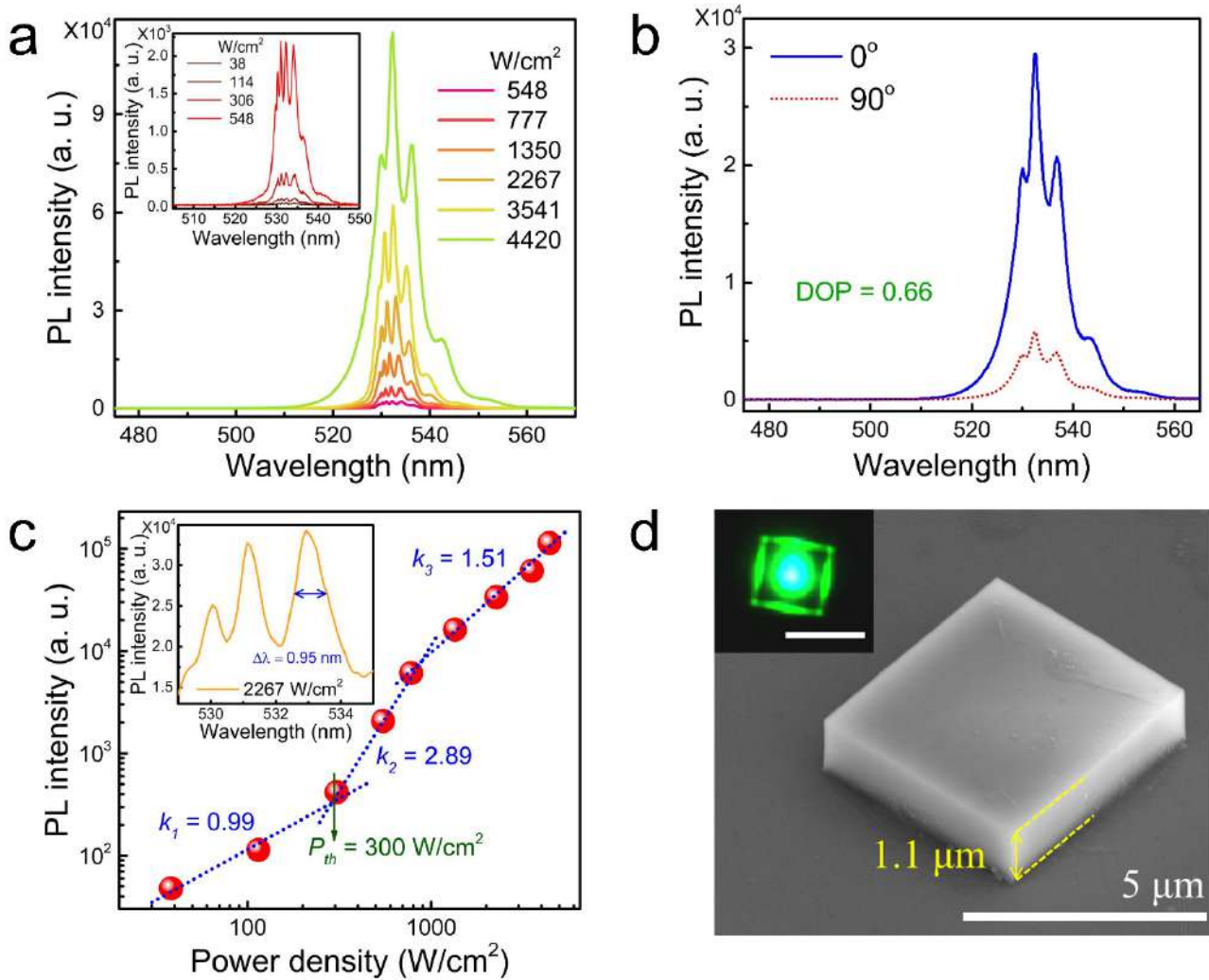


Figure S18 (a) PL spectra measured for the CsPbBr₃ SLs with $L = 4.5 \mu\text{m}$. The inset shows PL spectra of the CsPbBr₃ SL measured at an excitation power densities ranging from 38 to 548 W/cm^2 . (b) Emission polarization spectrum of the CsPbBr₃ SL. The degree of polarization (DOP) can be defined as $\text{DOP} = (I_{\text{max}} - I_{\text{min}}) / (I_{\text{max}} + I_{\text{min}})$ [1], and the value is calculated as 0.66. (c) Dependence of the PL intensity on the excitation power density. The inset shows the magnified spectrum of polariton mode measured at an excitation power density of 2267 W/cm^2 . (d) The SEM image of a $4.5 \mu\text{m}$ CsPbBr₃ SL with the thickness of $1.1 \mu\text{m}$ on a Ag film surface. The inset shows the optical image of the CsPbBr₃ SL. The length of the scale bar is $5 \mu\text{m}$.

References

- [1] H. Zhang, C. Zhao, S. Chen, J. Tian, J. Yan, G. Weng, X. Hu, J. Tao, Y. Pan, S. Chen, H. Akiyama, J. Chu, *Chem. Eng. J.*, 2020, **389**, 124395.
- [2] A. Kanevce, D. H. Levi, D. Kuciauskas, *Prog. Photovolt Res. Appl.*, 2014, **22**, 1138.
- [3] T. J. S. Evans, A. Schlaus, Y. Fu, X. Zhong, T. L. Atallah, M. S. Spencer, L. E. Brus, S. Jin, X. Y. Zhu, *Adv. Opt. Mater.*, 2018, **6**, 1700982.
- [4] J. Song, Q. Shang, X. Deng, Y. Liang, C. Li, Xi. Liu, Q. Xiong, Q. Zhang, *Adv. Mater.*, 2023, **35**, 2302170.